

**DISCRETE INVERSE WAVELETS TRANSFORM ANALYSIS
FOR GAS-SOLID TWO PHASE FLOW
—Extraction of Regular Particle Movements in Spiral Flow—**

Masahiro TAKEI	<i>Nihon University, Tokyo Japan</i>
Hui LI	<i>Kagoshima University, Kagoshima Japan</i>
Yao-Hua ZHAO	<i>University of Tokyo, Tokyo Japan</i>
Mitsuaki OCHI	<i>Nihon University, Tokyo Japan</i>
Yoshifuru SAITO	<i>Hosei University, Tokyo Japan</i>
Kiyoshi HORII	<i>Shirayuri Women's College, Tokyo Japan</i>

ABSTRACT

Two dimensional directions of regular particle movements in two phase spiral flow have been clearly extracted after reducing irregular particle movements by means of discrete wavelets transform and its multiresolution analysis. The method is composed of three steps. Firstly, the two dimensional vector data of all particles velocities on a cross section are transformed to the wavelets spectrum by the discrete wavelets transform. Secondly, the wavelets spectrum data are inversely transformed to each multiresolution level by means of the discrete inverse wavelets transform. Finally, after some multiresolution levels including the irregular data are reduced, the other levels are added each other, resulting in extracting the regular data that indicate two dimensional directions of the regular particle movements. The motivation behind this work is to make clear the relation between the air velocity distribution and the particle velocity distribution in the two phase spiral flow in order to improve the performance of the pneumatic transportation system using spiral flow. This study has tried applying the inverse method to analyzing the relation, that is to estimate the air velocity distribution from the particle movement in the spiral flow. This paper focuses on the extraction of the regular particle movements in the spiral flow as a preliminary study to achieve estimating the air velocity distribution.

INTRODUCTION

The high performance pneumatic transportation system using spiral flow which has a steep axial velocity profile and swirling motion with large free vortex region was preliminarily developed¹⁾. The rotating particles in this transportation system tend not to touch the pipe inner wall because the particles obtain high centripetal force from the spiral flow with the steep axial velocity distribution. The system is useful for the pneumatic transportation of fragile and viscous materials in chemical and food industries because of avoiding from material breaking and sticking to the pipe inner wall.

It is important to make clear the relation between the air velocity distribution and the particle velocity distribution in the two phase spiral flow to improve the system performance. The orderly analysis to estimate the particles movement from the air velocity distributions has been used in order to analyze the relation²⁾. Nowadays, inverse problems have been treated in the other fields such as material engineering³⁾. We have applied the idea of the inverse problem to analyzing the two phase spiral flow, that is, to estimate the air velocity distributions from the particles movement inversely. The inverse analysis has two aspects, which are the extraction of the regular particle movements, and the estimate of the air velocities from the extracted particles velocities. This paper focuses on the extraction of the regular particle movements in the spiral flow at the first aspects as a preliminary study. The originality of this paper lies in applying discrete wavelets transform and its multiresolution analysis to the two dimensional vector data in the two phase spiral flow in order to achieve the inverse problem.

Wavelets transform⁴⁾ is roughly classified with two types, which are continuous wavelets transform and discrete wavelets transform. The continuous wavelets transform has been generally used for time frequency analysis in vibration wave. The analysis enables to analyze simultaneously time and frequency and to extract peculiar points. Li classified eddy frequency passing in jet flow⁵⁾. On the other hand, the discrete wavelets transform has been mainly used for picture image processing. The analysis enables to compress picture image data and to extract peculiar points of the picture image data. Saito applied the idea to analyzing the electromagnetic wave⁶⁾. In this paper, the velocities of rotating particles on a cross section in the two phase spiral flow are measured. Next, the directions of the regular particle movements are extracted from the velocities after reducing the irregular particle movements by means of discrete wavelets transform and its multiresolution analysis.

EXPERIMENTS

Nozzle to Produce Spiral Flow & its Characteristics

The nozzle to produce the spiral flow is designed with an annular slit connecting to a conical cylinder as shown in Fig. 1⁷⁾. Pressurized air is forced through the sides of the device into the buffer area, and then through the annular slit into a vertical pipe entrance. The suction force is generated at the back of the nozzle by Coanda effect. The annular jet, passing through the conical cylinder, develops a spiral structure with a steeper axial velocity and an azimuthal velocity distributions, even if it is not applied tangentially⁸⁾. Particles at the back of the nozzle are sucked into the nozzle to be issued to the pipe as rotating.

The characteristics of the single phase spiral flow has been reported⁹⁾. According to the paper, the divergence angle of the spiral flow issued from the nozzle outlet is reduced 45 %, from 14.3 degrees to 7.8 degrees as compared with typical turbulence flow. The turbulent fluctuation level of the spiral flow is decreased about 55%, from 0.20 to 0.09 as compared with that of the typical turbulence flow. These results clearly indicates the focusing characteristic and the high stability of the spiral flow. The particles in the two phase spiral flow obtain high centripetal force.

Experimental Equipment, Method & Conditions

The experimental equipment consisted of a vertical acrylic pipe, the nozzle to produce the spiral flow, a CCD camera and an air compressor as shown in Fig. 2. The inside diameter of the vertical pipe is 41.0 mm and the height of the pipe is 1.5 m. The CCD camera to focus on a two dimensional cross section of the vertical pipe is set up at the top of the vertical pipe to record the particles trajectories.

With the experimental equipment, the movement of balls in the spiral flow on a two dimensional cross section are observed. The balls rotate inside the cross section of the vertical pipe when the gravity on the ball is well balanced with the drag force due to the upward velocity component of the spiral air flow.

The styrofoam balls are sucked from the intake part of the nozzle. The diameters of the balls are 6 mm and the specific gravity value is 700 kg/m³. The air flow rate is 8.7 X10⁻² m³/min. The mean velocity of the air flow in the vertical pipe calculated from the flow rate is 1.1 m/s. The Reynolds number calculated from the velocity is 3.0X10³.

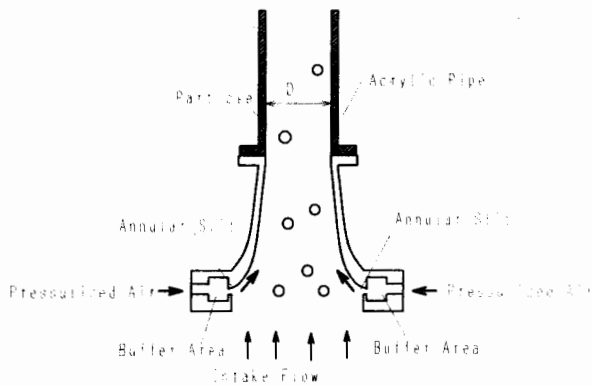


Fig. 1 Spiral flow nozzle

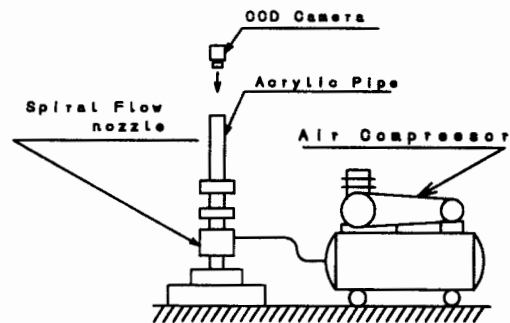
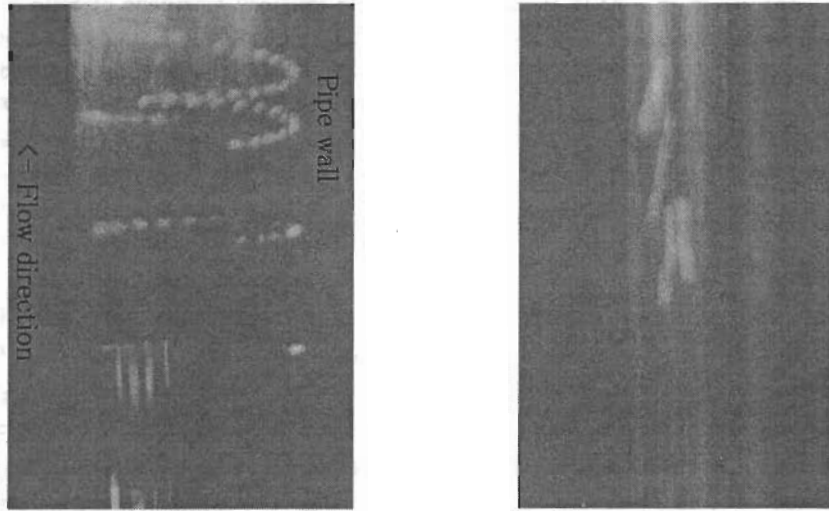


Fig. 2 Experimental equipment

Experimental Results

As a pre-experiment to clarify the ball movement in the two phase spiral flow as compared with that in the typical turbulence flow, several styrofoam balls movements are observed from the side of the vertical pipe on the above experimental conditions. The balls in the spiral flow rotated on a cross section of the vertical pipe at 0.8 m height from the outlet of the nozzle without touching the pipe inner wall as shown in Fig. 3 (a). The flow direction in the figure is upward. The balls had the balance between the gravity and the drag force. If the flow rate gets larger, the balls moved up as rotating. On the other hand, the balls in the typical turbulence flow moved randomly upward and downward as colliding the pipe inner wall as shown in Fig. 3 (b).

Next, plenty of styrofoam balls movements in the spiral flow are observed from the top of the vertical pipe on the above experimental conditions. The two dimensional velocity vector of the balls on the cross at a moment are acquired from the recorded particles trajectories. An example of the velocity vector at a moment is shown in Fig. 4. In this figure, the positions of the vector data are replaced to a rectangle cross section consisting 16X16 grids to simplify the further analysis. The length of the vector indicates the magnitude of the particle velocity, and the direction of the vector indicates the two dimensional direction of the particle movement at the moment. From the figure, the balls rotate counter-clockwise. Some particles move irregularly due to the wake and the collision and so on. For example, a particle located (10, 4) moves upwards; however, other particles around the particle move right upwards.



(a) Particles movements in spiral flow (b) Particles movements in turbulence flow
Fig. 3 Particles movements in spiral flow and turbulence flow

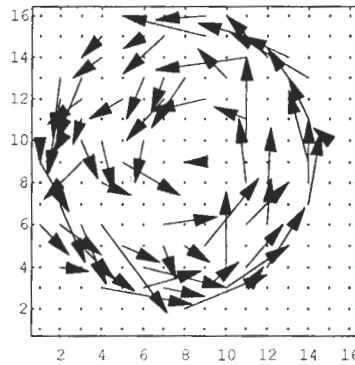


Fig. 4 Two dimensional velocity vector of particles in spiral flow

DISCRETE WAVELETS TRANSFORM ANALYSIS AND DISCUSSION

Outline of Wavelets Transform

The continuous wavelets transform $WT(b, a)$ of a real square integrable function $f(x)$ is defined as⁴⁾

$$WT(b, a) = \frac{1}{\sqrt{|a|}} \int_{-\infty}^{\infty} f(x) \overline{\phi\left(\frac{x-b}{a}\right)} dx \quad \text{---(1)}$$

Where, $f(x)$ is a target function with regard to one dimensional space x such as vibration data and image data, a is a scale variable, b is a location variable, and $\phi(x)$ is a real integrable analyzing wavelets with zero at large x and at small x . The function $f(x) \in L^2(R)$ at a location b and a scale a . $L^2(R)$ denotes Hilbert space. $\phi((x-b)/a)$ is a function to scale $\phi(x)$ by a times in x direction and to translate it by b . $\phi(x)$ is satisfied with the next admissible condition,

$$\int_{-\infty}^{\infty} \phi(x) dx = 0 \quad \text{---(2)}$$

From Eq. (1), after the scale variable a and the location variable b change to the discrete values; $a = 2^j$ and $b = 2^j k$ (j and k are integers), the discrete wavelets transform is expressed by

$$WT_k^{(j)} = 2^{\frac{j}{2}} \int_{-\infty}^{\infty} f(x) \overline{\phi(2^j x - k)} dx \quad \text{---(3)}$$

$\phi(2^j x - k)$ can be an orthonormal function when $\phi(x)$ is a special function. From Eq. (3), the discrete inverse wavelets transform is expressed by

$$f(x) = \sum_{j=-\infty}^{\infty} \sum_{k=-\infty}^{\infty} WT_k^{(j)} \phi(2^j x - k) \quad \text{---(4)}$$

Eq. (3) becomes simple matrix operations when the elements of $f(x)$ is composed of discrete values. When the sampling number in terms of $f(x)$ in x direction is n (n is a second exponent value), a matrix \mathbf{X} that indicates $f(x)$ in Eq. (3) has the sampling data. The wavelets spectrum matrix \mathbf{S} that indicates $WT_k^{(j)}$ in Eq. (3) is obtained from

$$\mathbf{S} = \mathbf{W}_n \cdot \mathbf{X} \quad \text{---(5)}$$

Where, \mathbf{W}_n is a discrete analyzing wavelets matrix that indicates $\phi(2^j x - k)$ in Eq. (3). In this analysis, four dimensional Daubechies function is used as the analyzing wavelets. The analyzing wavelets is an orthonormal function. The analyzing wavelets matrix \mathbf{W}_n is acquired by a cascade algorithm on the basis of a scaling function matrix \mathbf{C} . The scaling function is shown in Eq. (6).

$$\mathbf{C} = \begin{pmatrix} c_0 & c_1 & c_2 & c_3 & 0 & 0 & \cdot & 0 & 0 & 0 & 0 \\ c_3 & -c_2 & c_1 & -c_0 & 0 & 0 & \cdot & 0 & 0 & 0 & 0 \\ 0 & 0 & c_0 & c_1 & c_2 & c_3 & \cdot & 0 & 0 & 0 & 0 \\ 0 & 0 & c_3 & -c_2 & c_1 & -c_0 & \cdot & 0 & 0 & 0 & 0 \\ \cdot & \cdot & \cdot & \cdot & \cdot & \cdot & \cdot & \cdot & \cdot & \cdot & \cdot \\ 0 & 0 & 0 & 0 & 0 & 0 & \cdot & c_0 & c_1 & c_2 & c_3 \\ 0 & 0 & 0 & 0 & 0 & 0 & \cdot & c_3 & -c_2 & c_1 & -c_0 \\ c_2 & c_3 & 0 & 0 & 0 & 0 & \cdot & 0 & 0 & c_0 & c_1 \\ c_1 & -c_0 & 0 & 0 & 0 & 0 & \cdot & 0 & 0 & c_3 & -c_2 \end{pmatrix} \begin{matrix} c_0 = \frac{1+\sqrt{3}}{4\sqrt{2}} \\ c_1 = \frac{3+\sqrt{3}}{4\sqrt{2}} \\ c_2 = \frac{3-\sqrt{3}}{4\sqrt{2}} \\ c_3 = \frac{1-\sqrt{3}}{4\sqrt{2}} \end{matrix} \quad \text{---(6)}$$

$$c_3 - c_2 + c_1 - c_0 = 0 \quad \text{---(7)} \quad 0 c_3 - 1 c_2 + 2 c_1 - 3 c_0 = 0 \quad \text{---(8)}$$

Where, $\mathbf{C}^T \cdot \mathbf{C} = \mathbf{I}$, \mathbf{I} is a unit matrix and \mathbf{C}^T is a transpose matrix of \mathbf{C} . In Eq. (6), the first line shows a transform to get the mean values to put the weights of c_0, c_1, c_2 and c_3 on the input data. The second line shows a transform to get the difference values to put the weights of c_0, c_1, c_2 and c_3 on the input data. The third line shows a transform to translate the first line by two steps in x direction. The fourth line is a transform to do the second line by two steps. Eqs. (7) and (8) show the transformed values are zero when the input data are constant or simply increased. To explain easily the process to acquire the analyzing wavelets matrix \mathbf{W}_n from \mathbf{C} , the matrix \mathbf{X} is defined as one dimensional 16 elements,

$$\mathbf{X} = [x_1 x_2 x_3 x_4 x_5 x_6 x_7 x_8 x_9 x_{10} x_{11} x_{12} x_{13} x_{14} x_{15} x_{16}]^T \quad \text{---(9)}$$

From Eqs. (6) and (9), the transformed matrix \mathbf{X}' is

$$\mathbf{X}' = \mathbf{C}_{16} \mathbf{X} = [s_1 d_1 s_2 d_2 s_3 d_3 s_4 d_4 s_5 d_5 s_6 d_6 s_7 d_7 s_8 d_8]^T \quad \text{---(10)}$$

Where, \mathbf{C}_{16} is 16X16 matrix of \mathbf{C} . The element s indicates the mean value and the element d indicates the difference value. The elements in the matrix \mathbf{X}' are replaced by a matrix \mathbf{P}_{16} .

$$\mathbf{P}_{16} \mathbf{X}' = \mathbf{P}_{16} \mathbf{C}_{16} \mathbf{X} = [s_1 s_2 s_3 s_4 s_5 s_6 s_7 s_8 d_1 d_2 d_3 d_4 d_5 d_6 d_7 d_8]^T \quad \text{---(11)}$$

Where, \mathbf{P}_{16} is defined as

$$\mathbf{P}_{16} = \begin{pmatrix} 1 & 0 & 0 & 0 & 0 & 0 & 0 & 0 & 0 & 0 & 0 & 0 & 0 & 0 & 0 & 0 \\ 0 & 0 & 1 & 0 & 0 & 0 & 0 & 0 & 0 & 0 & 0 & 0 & 0 & 0 & 0 & 0 \\ 0 & 0 & 0 & 0 & 1 & 0 & 0 & 0 & 0 & 0 & 0 & 0 & 0 & 0 & 0 & 0 \\ 0 & 0 & 0 & 0 & 0 & 0 & 1 & 0 & 0 & 0 & 0 & 0 & 0 & 0 & 0 & 0 \\ 0 & 0 & 0 & 0 & 0 & 0 & 0 & 0 & 1 & 0 & 0 & 0 & 0 & 0 & 0 & 0 \\ 0 & 0 & 0 & 0 & 0 & 0 & 0 & 0 & 0 & 0 & 1 & 0 & 0 & 0 & 0 & 0 \\ 0 & 0 & 0 & 0 & 0 & 0 & 0 & 0 & 0 & 0 & 0 & 0 & 1 & 0 & 0 & 0 \\ 0 & 0 & 0 & 0 & 0 & 0 & 0 & 0 & 0 & 0 & 0 & 0 & 0 & 0 & 1 & 0 \\ 0 & 1 & 0 & 0 & 0 & 0 & 0 & 0 & 0 & 0 & 0 & 0 & 0 & 0 & 0 & 0 \\ 0 & 0 & 0 & 1 & 0 & 0 & 0 & 0 & 0 & 0 & 0 & 0 & 0 & 0 & 0 & 0 \\ 0 & 0 & 0 & 0 & 0 & 1 & 0 & 0 & 0 & 0 & 0 & 0 & 0 & 0 & 0 & 0 \\ 0 & 0 & 0 & 0 & 0 & 0 & 0 & 1 & 0 & 0 & 0 & 0 & 0 & 0 & 0 & 0 \\ 0 & 0 & 0 & 0 & 0 & 0 & 0 & 0 & 1 & 0 & 0 & 0 & 0 & 0 & 0 & 0 \\ 0 & 0 & 0 & 0 & 0 & 0 & 0 & 0 & 0 & 0 & 1 & 0 & 0 & 0 & 0 & 0 \\ 0 & 0 & 0 & 0 & 0 & 0 & 0 & 0 & 0 & 0 & 0 & 0 & 1 & 0 & 0 & 0 \\ 0 & 0 & 0 & 0 & 0 & 0 & 0 & 0 & 0 & 0 & 0 & 0 & 0 & 0 & 1 & 0 \\ 0 & 0 & 0 & 0 & 0 & 0 & 0 & 0 & 0 & 0 & 0 & 0 & 0 & 0 & 0 & 1 \end{pmatrix} \quad \text{---(12)}$$

Moreover, from Eq. (11), the transform is carried out by \mathbf{C} and \mathbf{P} ,

$$\mathbf{W}^{(2)} \mathbf{X} = [S_1 S_2 S_3 S_4 D_1 D_2 D_3 D_4 d_1 d_2 d_3 d_4 d_5 d_6 d_7 d_8]^T \quad \text{---(13)}$$

$$\mathbf{S} = \mathbf{W}^{(3)} \mathbf{X} = [S_1 S_2 D_1 D_2 D_1 D_2 D_3 D_4 d_1 d_2 d_3 d_4 d_5 d_6 d_7 d_8]^T \quad \text{---(14)}$$

Where,

$$\mathbf{W}^{(2)} = (\mathbf{P}_{16}' \mathbf{C}'_{16}) (\mathbf{P}_{16} \mathbf{C}_{16}) \quad \text{---(15)} \quad \mathbf{W}^{(3)} = (\mathbf{P}_{16}'' \mathbf{C}_{16}') (\mathbf{P}_{16}' \mathbf{C}_{16}') (\mathbf{P}_{16} \mathbf{C}_{16}) \quad \text{---(16)}$$

$$\mathbf{P}_{16}' = \begin{bmatrix} \mathbf{P}_8 & \mathbf{0} \\ \mathbf{0} & \mathbf{I}_8 \end{bmatrix} \quad \mathbf{C}_{16}' = \begin{bmatrix} \mathbf{C}_8 & \mathbf{0} \\ \mathbf{0} & \mathbf{I}_8 \end{bmatrix} \quad \mathbf{P}_{16}'' = \begin{bmatrix} \mathbf{P}_4 & \mathbf{0} \\ \mathbf{0} & \mathbf{I}_{12} \end{bmatrix} \quad \mathbf{C}_{16}'' = \begin{bmatrix} \mathbf{C}_4 & \mathbf{0} \\ \mathbf{0} & \mathbf{I}_{12} \end{bmatrix} \quad \text{---(17)}$$

$\mathbf{W}^{(3)}$ is a analyzing wavelets matrix that is \mathbf{W}_n in Eq. (5). The wavelets spectrum \mathbf{S} in Eq. (5) is $\mathbf{W}^{(3)} \mathbf{X}$ in Eq. (14).

In Eq. (13), S_i indicates the mean value from s_i to s_j in Eq. (11). S_2 indicates the mean value from s_3 to s_6 that translate by two steps. D_1 indicates the difference value from s_i to s_j . In Eq. (14), S_1 indicates the mean value from S_i to S_j in Eq. (13). D_1 indicates the difference value from S_i to S_j in Eq. (13). From Eq. (14), the input data are transformed to the mean value and difference value with valuable resolution levels by the discrete wavelets transform. The input data in the space are divided into the range from high frequency to low

frequency.

From Eqs. (5) and (14), the inverse wavelets transform is,

$$\mathbf{X} = \mathbf{W}_n^T \mathbf{S} = [\mathbf{W}^{(3)}]^T \mathbf{S} \quad \text{---(18)}$$

$$[\mathbf{W}^{(3)}]^T = [(\mathbf{P}_{16}'' \mathbf{C}_{16}'')(\mathbf{P}_{16}' \mathbf{C}_{16}')(\mathbf{P}_{16} \mathbf{C}_{16})]^T = \mathbf{C}_{16}^T \mathbf{P}_{16}^T (\mathbf{C}_{16}')^T (\mathbf{P}_{16}')^T (\mathbf{C}_{16}'')^T (\mathbf{P}_{16}'')^T \quad \text{---(19)}$$

In Eq. (5), one dimensional space is replaced with two dimensional space in x and y directions. When the sampling number in x direction is n and that in y direction is m (n and m are second exponent values), a matrix \mathbf{H} ($n \times m$) has the sampling data. The two dimensional wavelets spectrum \mathbf{S} is obtained from

$$\mathbf{S} = \mathbf{W}_n \cdot \mathbf{H} \cdot \mathbf{W}_m^T \quad \text{---(20)}$$

Where, \mathbf{W}_m^T is a transpose matrix of \mathbf{W}_m .

In this analysis, because the data located at each grid in Fig. 4 are vector data, x component and y component are calculated separately in Eq. (20). The two dimensional wavelets spectrum of x component of the vector data \mathbf{S}_x and that of y component \mathbf{S}_y are obtained from

$$\mathbf{S}_x = \mathbf{W}_n \cdot \mathbf{H}_x \cdot \mathbf{W}_m^T \quad \mathbf{S}_y = \mathbf{W}_n \cdot \mathbf{H}_y \cdot \mathbf{W}_m^T \quad \text{---(21)}$$

Where, \mathbf{H}_x and \mathbf{H}_y are $n \times m$ matrixes to show x and y components of the velocity vector data. The elements of the matrix show the velocities on the grid of the particle position in Fig. 4. From Eq. (21), the discrete inverse wavelets transform is expressed by

$$\mathbf{H}_x = \mathbf{W}_n^T \cdot \mathbf{S}_x \cdot \mathbf{W}_m \quad \mathbf{H}_y = \mathbf{W}_n^T \cdot \mathbf{S}_y \cdot \mathbf{W}_m \quad \text{---(22)}$$

In this analysis, $n=16$ and $m=16$ as shown in Fig. 4.

Assumptions for Analysis

The following assumptions and prior conditions are set up. (1) The air velocity V_a at a moment is

$$V_a = V_p + V'(d, Re, \nu_d / \nu_p)$$

Where, V_p is particle velocity and V' is additional velocity on a particle. When $d/L(Re) < 1$ and $\nu_d / \nu_p = 1$, $V' = 0$. L is characteristic eddy length, d is particle diameter, Re is Reynolds number, ν_a is air viscosity and ν_p is particle viscosity. In this analysis, the particles do not follow the air movement because of $V' \neq 0$. (2) The particle velocity distribution at a moment in Fig. 4 is treated. (3) A two-dimensional cross section of the vertical pipe is considered. Namely, the z direction is ignored. (4) The velocity at a grid without any particles is assumed to be zero in Fig. 4.

Analysis Method

This analysis consists of three steps. Firstly, the two dimensional vector data of the particles velocities in Fig. 4, \mathbf{H}_x and \mathbf{H}_y , are respectively transformed to the wavelets spectrum \mathbf{S}_x and \mathbf{S}_y by means of the discrete wavelets transform in x and y components in Eq. (21).

Next, the multiresolution analysis can be carried out because the wavelets transform is a orthonormal transform, that is, each part of the spectrum is inversely transformed to five multiresolution levels by means of the discrete inverse wavelets transform. From Eq. (18), to explain easily, the multiresolution analysis about one dimensional data is,

$$\mathbf{X} = [\mathbf{W}^{(3)}]^T \mathbf{S} = [\mathbf{W}^{(3)}]^T \mathbf{S}_1 + [\mathbf{W}^{(3)}]^T \mathbf{S}_2 + [\mathbf{W}^{(3)}]^T \mathbf{S}_3 + [\mathbf{W}^{(3)}]^T \mathbf{S}_4 + [\mathbf{W}^{(3)}]^T \mathbf{S}_5 \quad \text{---(23)}$$

Where,

$$\begin{aligned} \mathbf{S}_1 &= [S_1 \ 0 \ 0 \ 0 \ 0 \ 0 \ 0 \ 0 \ 0 \ 0 \ 0 \ 0 \ 0 \ 0 \ 0 \ 0]^T & \mathbf{S}_2 &= [0 \ S_2 \ 0 \ 0 \ 0 \ 0 \ 0 \ 0 \ 0 \ 0 \ 0 \ 0 \ 0 \ 0 \ 0 \ 0]^T \\ \mathbf{S}_3 &= [0 \ 0 \ D_1 \ D_2 \ 0 \ 0 \ 0 \ 0 \ 0 \ 0 \ 0 \ 0 \ 0 \ 0 \ 0 \ 0]^T & \mathbf{S}_4 &= [0 \ 0 \ 0 \ 0 \ D_1 \ D_2 \ D_3 \ D_4 \ 0 \ 0 \ 0 \ 0 \ 0 \ 0 \ 0 \ 0]^T \\ \mathbf{S}_5 &= [0 \ 0 \ 0 \ 0 \ 0 \ 0 \ 0 \ 0 \ d_1 \ d_2 \ d_3 \ d_4 \ d_5 \ d_6 \ d_7 \ d_8]^T \end{aligned} \quad \text{---(24)}$$

In Eq. (22), the first term is Level 1, the second term is Level 2. The further terms are the same process. The resolution gets double higher as the level increases. Fig. 5 shows a model of a wavelets spectrum to explain the method of the multiresolution analysis in two dimensional space. In detail, 1X1 part in the wavelets spectrum inversely transforms to Level 1 with Eq. (22) after the outside is replaced to zero. The inverse transform is carried out separately in x and y components of the particle velocity. Next, the inside of 2X2 parts in the spectrum inversely transform to Level 2 after the outside and the 1X1 part are replaced to zero. The further process is the same, the inside of 4X4 parts in the spectrum except for the inside of 2X2 parts inversely transform to Level 3. The inside of 8X8 parts in the spectrum except for the inside of 4X4 parts inversely transform to Level 4. The inside of 16X16 parts in the spectrum except for the inside of 8X8 parts inversely transform to Level 5.

Finally, each level except for the level including the random vector are added to obtain the direction of the regular particles, because the random vector on the level is caused by the effect of the irregular particles.

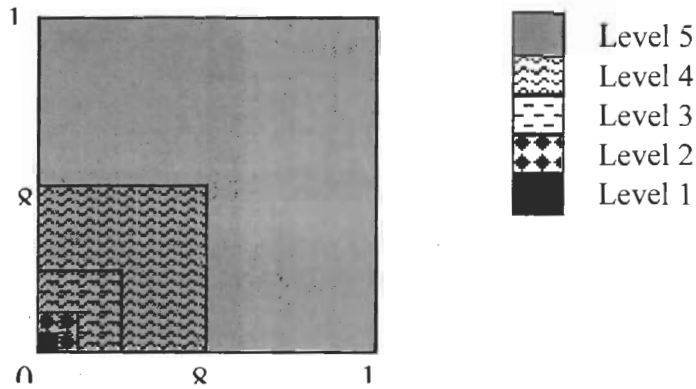


Fig. 5 Method of multiresolution from wavelets spectrum

Analysis Results & Discussion

Figs. 6 (a) and (b) show the wavelets spectrum of x and y components of the particles velocities by means of the discrete wavelets transform in Eq. (22). In these figures, the whiter parts at each grid show the larger transformed values, the darker parts show the lower transformed values. In this analysis, the transformed data are separated from the low frequency level to high frequency level by the discrete wavelets transform. The low frequency level that is the whole means values of the original particles velocities data concentrate on the inside of 2×2 parts. The lower middle frequency level concentrates on the inside of 4×4 parts in the spectrum. The higher middle frequency level concentrates on the inside of 8×8 parts in the spectrum. The high frequency level that is the difference values among four particles each other collects inside 16×16 parts in the spectrum.

Fig. 7 shows the results of the multiresolution analysis from transforming inversely each part of the wavelets spectrum in Fig. 6. Fig. 7 (a) shows the mean direction of all particles. That is obtained from transforming inversely the mother wavelets vector (1×1) . Fig. 7 (b) is Level 2, that is, to show the mean directions of the particles divided by four parts. Fig. 7 (c) indicates the mean direction with lower middle frequency level. At this level, the directions indicates swirling motion on the whole. Fig. 7 (d) indicates the mean direction with higher middle frequency level. This level has the random vector. Fig. 7 (e) is level 5 to show the mean direction with high level frequency. This level includes the larger random vector.

From this multiresolution, the spectrum can be divided from low frequency level to high frequency level. The resolution gets half as level increases by one step. Adding from level 1 to level 5, the original velocity vector in Fig. (4) is recovered.

Adding from Level 1 to Level 4 results in Fig. 8 (a) after reducing Level 5, because Level 5 shows the random vector. Adding from Level 1 to Level 3 results in Fig. 8 (b). Fig. 8 (b) shows the regular particle movements more clearly than Fig. 8 (a). From these figures, the regular particles movements are clearly extracted.

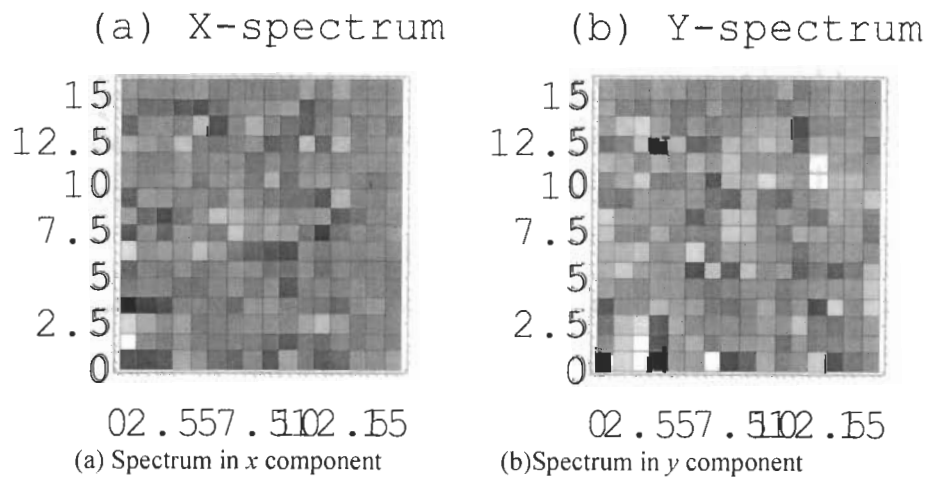


Fig. 6 Wavelets spectrum from particle velocity

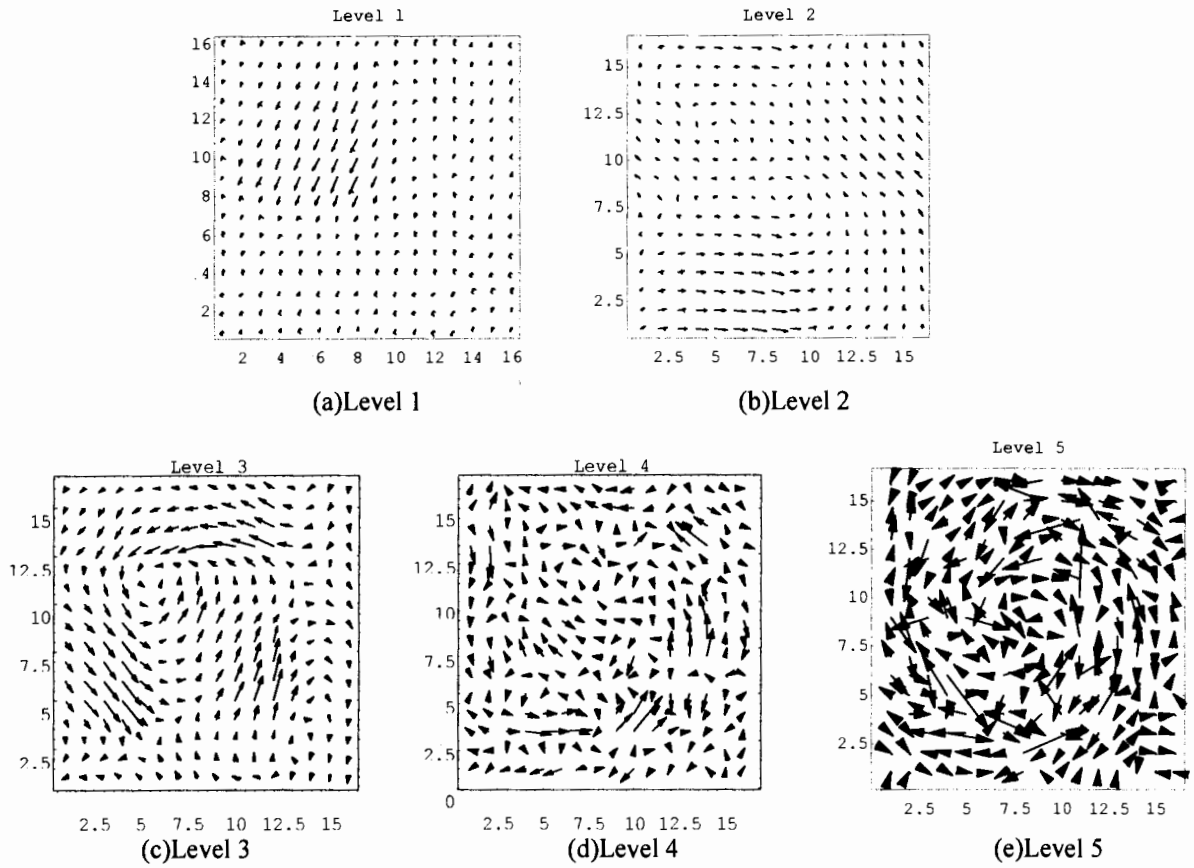


Fig. 7 Multiresolution analysis

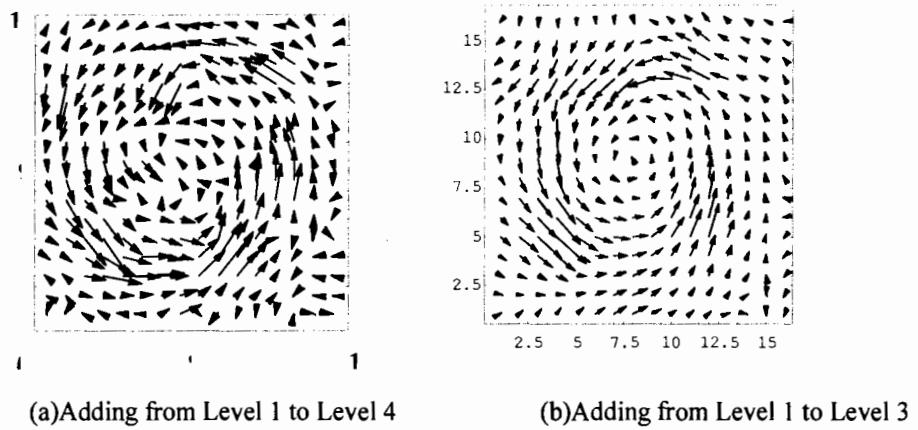


Fig. 8 Regular particle movement direction in spiral flow

CONCLUSIONS

Two dimensional directions of regular particle movements in spiral flow have been clearly extracted by means of discrete wavelets transform and its multiresolution analysis. The method is composed of three steps, which are the discrete wavelets transform of the particle velocity, the inverse transform to each multiresolution level, and reduction of the irregular data resulting in extracting the regular data. The velocity data in two dimensional space can be divided from low frequency level to high frequency level because the wavelets transform is orthonormal transform. This results lead to a new idea to estimate the air velocity from the particle velocity inversely.

ACKNOWLEDGEMENTS

The authors are pleased to acknowledge the considerable assistance of Mr. T. Katayanagi in Nihon University. This study is supported by the Mikiya foundation in Japan.

REFERENCES

- 1)Takei,M. Ochi,M., Horii,K. and Zhao,Y., Transporting Particles without Touching Pipe Wall, *ASME FED, FEDSM97-3629*(1997)
- 2)Tsuji,Y., Discrete Particle Simulation of Gas-solid Flows (From dilute to dense flows) Review, *KONA*, 11, 57 (1993)
- 3) Kubo,S., Inverse Problem Related to the Mechanics and Fracture of Solids and Structures, *JSME Int. J. Ser.1*, Vol.31, No.2, pp157-166 (1988)
- 4)Molet.J. et.al Wavelet Propagation and Sampling Theory, *Geophysics*, Vol.11, (1989)
- 5)Li, H., Wavelet Reynolds Stress Analysis of Two-Dimensional Vortex Flow, *ASME FEDSM97-3040* (1997)
- 6)Saito,Y., Wavelet Analysis for Computational Electromagnetics, (in Japanese), *Trans. IEE of Japan*, Vol. 116A, No10, pp833-839(1996)
- 7)Horii,K., 1988, *US.PAT. No.4,721,126, UK.PAT. No.2, 180, 957.*
- 8)Horii,K., Using Spiral Flow for Optical Cord Passing *Mechanical Engineering - ASME*, Vol.112, No.8, pp68-69 (1990)
- 9)Horii,K. et al., A Coanda Spiral Device Passing Optical Cords with Mechanical Connectors Attached through a Pipeline, *ASME FED-Vol.121, Gas-Solid Flows*, pp65-70. (1991)